The non-equilibrium response of a superconductor to pair-breaking radiation measured over a broad frequency band

de Visser, P. J.; Yates, S. J. C.; Guruswamy, T.; Goldie, D. J.; Withington, S.; Neto, A.; Llombart, N.; Baryshev, A. M.; Klapwijk, T. M.; Baselmans, J. J. A.

Published in:
Applied Physics Letters

DOI:
10.1063/1.4923097

The non-equilibrium response of a superconductor to pair-breaking radiation measured over a broad frequency band

P. J. de Visser, S. J. C. Yates, T. Guruswamy, D. J. Goldie, S. Withington, A. Neto, N. Llombart, A. M. Baryshev, T. M. Klapwijk, and J. J. A. Baselmans

Citation: Appl. Phys. Lett. **106**, 252602 (2015); doi: 10.1063/1.4923097
View online: https://doi.org/10.1063/1.4923097
View Table of Contents: http://aip.scitation.org/toc/apl/106/25
Published by the American Institute of Physics

The non-equilibrium response of a superconductor to pair-breaking radiation measured over a broad frequency band

P. J. de Visser,[1,a)] S. J. C. Yates,[2] T. Guruswamy,[3] D. J. Goldie,[3] S. Withington,[3] A. Neto,[4] N. Llombart,[4] A. M. Baryshev,[2,5] T. M. Klapwijk,[1,6] and J. J. A. Baselmans[7,4]
[1]*Kavli Institute of NanoScience, Faculty of Applied Sciences, Delft University of Technology, Lorentzweg 1, 2628 CJ Delft, The Netherlands*
[2]*SRON Netherlands Institute for Space Research, Landleven 12, 9747AD Groningen, The Netherlands*
[3]*Cavendish Laboratory, University of Cambridge, JJ Thomson Avenue, Cambridge CB3 0HE, United Kingdom*
[4]*Faculty of Electrical Engineering, Mathematics and Computer Science, Terahertz Sensing Group, Delft University of Technology, Mekelweg 4, 2628 CD Delft, The Netherlands*
[5]*Kapteyn Astronomical Institute, University of Groningen, Landleven 12, 9747 AD Groningen, The Netherlands*
[6]*Physics Department, Moscow State Pedagogical University, Moscow 119991, Russia*
[7]*SRON Netherlands Institute for Space Research, Sorbonnelaan 2, 3584 CA Utrecht, The Netherlands*

(Received 22 May 2015; accepted 16 June 2015; published online 25 June 2015)

We have measured the absorption of terahertz radiation in a BCS superconductor over a broad range of frequencies from 200 GHz to 1.1 THz, using a broadband antenna-lens system and a tantalum microwave resonator. From low frequencies, the response of the resonator rises rapidly to a maximum at the gap edge of the superconductor. From there on, the response drops to half the maximum response at twice the pair-breaking energy. At higher frequencies, the response rises again due to trapping of pair-breaking phonons in the superconductor. In practice, this is a measurement of the frequency dependence of the quasiparticle creation efficiency due to pair-breaking in a superconductor. The efficiency, calculated from the different non-equilibrium quasiparticle distribution functions at each frequency, is in agreement with the measurements. © *2015 AIP Publishing LLC*.
[http://dx.doi.org/10.1063/1.4923097]

In a superconductor at low temperature, most of the electrons are bound in Cooper pairs. These pairs can be broken into quasiparticles by absorbing photons with an energy larger than the binding energy. This mechanism is frequently used to detect submillimetre and terahertz radiation using conventional superconductors such as aluminium. Pair-breaking detectors are usually assumed to measure the number of quasiparticles created by the absorbed radiation. The observable that measures the number of quasiparticles varies from the complex conductivity for microwave kinetic inductance detectors[1] (MKIDs), the current through a tunnel junction[2] to the capacitance of a small superconducting island.[3] These observables are mainly sensitive to quasiparticles with an energy close to the gap energy of the superconductor, Δ. The working principle of these detectors is usually explained in terms of an effective number of quasiparticles, which is maintained by a balance between the radiation power and electron-phonon interaction (recombination).[4] To convert the power (P) into a number of quasiparticles (N_{qp}), the quasiparticle creation efficiency η_{pb} is introduced, which compares the actual N_{qp} with the maximum possible N_{qp} when all created quasiparticles would have an energy Δ. Since Cooper pairs have a binding energy of 2Δ, a photon with an energy in between 2Δ and 4Δ can still only create two quasiparticles. The rest of the energy is lost through electron-phonon scattering, hence, $\eta_{pb} < 1$. For higher energies, η_{pb} depends on the phonon trapping factor, which determines whether high energy phonons are directly lost or can break an additional pair. η_{pb} is therefore not an efficiency in the sense that photons are lost, but it reduces the detector responsivity. MKIDs are superconducting microwave resonators which sense the number of quasiparticles through the complex conductivity of the superconductor. The phase response (θ) of such a resonator can be approximated by

$$\theta \propto -\frac{\delta\sigma_2}{\sigma_2} \propto \delta N_{qp} \propto \eta_{pb} P, \tag{1}$$

where σ_2 is the imaginary part of the complex conductivity. For the last proportionality, we assume to be in the linear regime where the quasiparticle recombination lifetime does not change significantly upon a change in N_{qp}. N_{qp} is dominated by background power and $\delta N_{qp} \ll N_{qp}$. η_{pb}, and hence the detector response, is dependent on the frequency of the absorbed photons, even at constant absorbed power.

On a microscopic level, the pair-breaking radiation leads to injection of quasiparticles at very specific energies.[5] Together with electron-phonon interaction (scattering and recombination),[6] a non-equilibrium, non-thermal quasiparticle energy distribution $f(E)$ is formed, which determines the response to pair-breaking radiation, as recently shown in Ref. 7. For microwave resonators, this is reflected in the explicit dependence of σ_2 on $f(E)$[8]

$$\frac{\sigma_2}{\sigma_N} = \frac{1}{\hbar\omega}\int_{\Delta-\hbar\omega}^{\Delta} \left[1 - 2f(E+\hbar\omega)\right] g_2(E) dE, \tag{2}$$

[a)]Electronic mail: p.j.devisser@tudelft.nl. Present address: Department of Quantum Matter Physics, University of Geneva, Geneva 1211, Switzerland.

$$g_2(E) = \frac{E^2 + \Delta^2 + \hbar\omega E}{(\Delta^2 - E^2)^{1/2}\left[(E+\hbar\omega)^2 - \Delta^2\right]^{1/2}}, \qquad (3)$$

where σ_N is the normal state conductivity, $\hbar$ is the reduced Planck's constant, and ω is the microwave frequency. η_{pb} is thus an attempt to capture all information contained in $f(E)$ in a single number, to allow for an effective quasiparticle number approach, as given by Eq. (1).

Here, we present a measurement of η_{pb} over a broad range in frequencies close to the superconducting gap (350–1100 GHz). A Ta MKID is used as the detector in a Fourier transform spectrometer (FTS) to measure the frequency dependence of the response. The measured response curve of the detector can be well explained by a frequency dependent η_{pb}, caused by a different non-equilibrium $f(E)$ calculated for different pair-breaking frequencies.

From an applied point of view, MKIDs[9] are considered promising detectors for large arrays due to the intrinsic ease of multiplexing their readout. MKIDs are photon noise limited for various frequencies.[10–15] The level of experimental detail that has now been achieved[13,16,17] calls for a more detailed understanding of the absorption of radiation. An important gap in this understanding is a measurement of η_{pb}. η_{pb} determines key parameters: The responsivity of the detector, the recombination noise level in the photon-noise limited regime,[10] and the sensitivity in the generation-recombination noise dominated limit.[18] The common number used for η_{pb} is 0.57 for all signal frequencies, which was derived for the temporal relaxation of very high energy excitations which first create a photo-electron,[19,20] an approach which is not applicable for frequencies close to the gap.

Previous studies of the absorption of radiation in superconductors have either measured $f(E)$ directly with tunnel-junctions,[21,22] but only with a single-frequency optical laser, or measured the absorption over a broad band with a bolometer,[23,24] which is insensitive to the non-equilibrium effects that determine η_{pb}. To measure η_{pb} over a broad frequency band, a known and relatively constant radiation power over a broad frequency band is required. Second, we need the absorption of all of that power at all frequencies within the volume of the detector to exclude the effect of frequency dependent absorption.[23] We therefore use a particularly wideband lens-antenna system, which is based on the leaky-wave antenna[25] and shown in Fig. 1. It consists of a 30 μm wide, 4 mm long slot, etched in a 200 nm thick Ta film with a resistivity of 6.7 $\mu\Omega$ cm, which is sputter deposited onto a 3 μm thick SiN membrane, and onto the surrounding substrate (Fig. 1(b)), using a 6 nm Nb seed layer. A spacer chip, placed in between the Ta film and the Si lens, ensures a 35 μm vacuum gap between the metal layer and the Si lens, which is crucial to get a high directivity of the antenna over a broad frequency band.[25,26] The membrane is required for the antenna, not for the MKID. This lens-antenna was demonstrated to have very clean beampatterns over the frequency range of 300–900 GHz. The antenna launches the signal as a travelling wave into a coplanar waveguide (CPW) with a central strip of 3.5 μm and slots of 3 μm wide, which length is designed to make a quarter wavelength resonator at 4.6571 GHz (the MKID detector). An extensive discussion of the design, fabrication process, and beampattern measurements can be found in Ref. 26.

The detector is cooled down in a ^{3}He/^{4}He cryostat to a bath temperature of 320 mK. The cryostat has optical access through a window, Goretex infrared blockers at 77 K and 4 K, and a 1.1 THz lowpass filter at 4 K. The Michelson FTS consists of a globar source at 2000 °C, a fixed and a movable mirror and a mylar beamsplitter. To eliminate absorption lines due to water, the FTS is placed in vacuum. The MKID itself is the detector in this setup. The phase response of the detector was measured as a function of the mirror distance. The phase response is linear in power, which is verified using the response to a full rotation of a polariser in a separate measurement (i.e., the last proportionality in Eq. (1) is valid). The Fourier transform of the interferogram, corrected for the frequency dependence of the filters and beamsplitter (see the supplementary Figure S1 (Ref. 27)), is shown in Fig. 2 as black dots, which is the central result of this letter. The

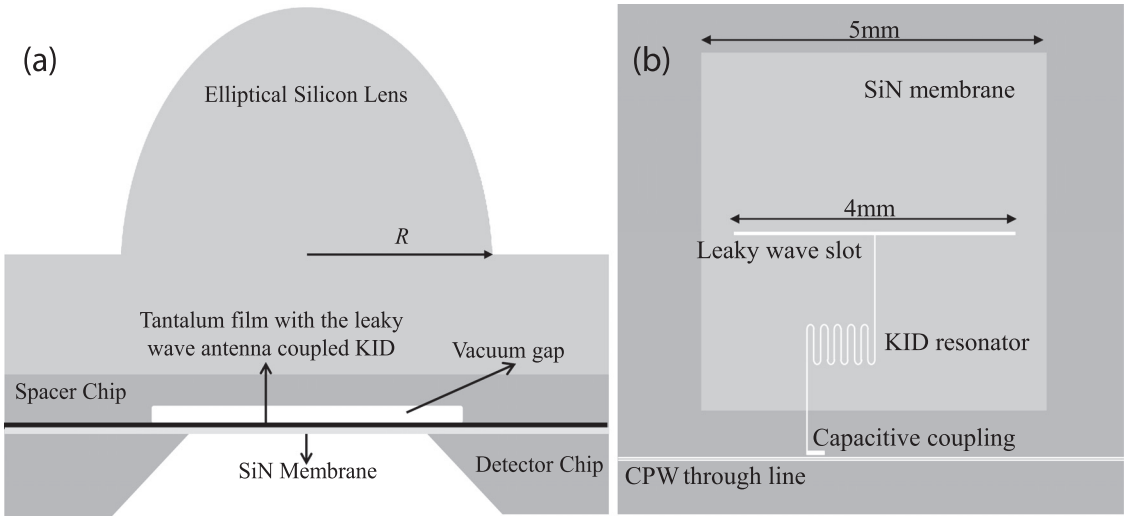

FIG. 1. (a) Schematic of the detector. The detector chip is fabricated on a SiN membrane and glued to an elliptical lens, leaving a small vacuum gap between the antenna and the lens-dielectric. (b) The design of the detector chip. The antenna slot, coupled to a microwave resonator, is fabricated on a SiN membrane (light grey square). The resonator is capacitively coupled to a microwave readout line.

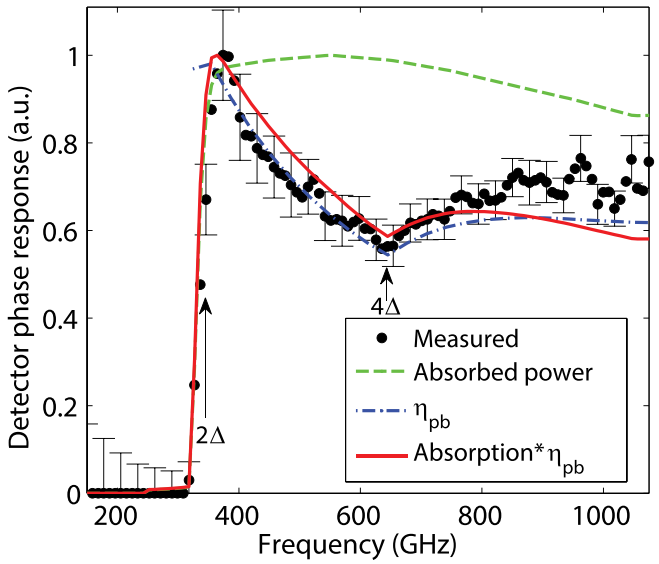

FIG. 2. The measured phase response (dots) of the microwave resonator as a function of the frequency of the pair-breaking radiation and normalised to one. Error bars are shown every third point. The green dashed line represents a calculation of the power absorption of the superconducting transmission line, including the antenna efficiency. The blue dashed-dotted line is a simulation of the pair-breaking efficiency (not normalised) that arises due to the different quasiparticle distributions at different excitation frequencies. The red line combines the two effects. The red and green lines are both normalised to one.

beamsplitter response contains a cross-polarisation contribution of 28% ± 5%, which is derived by integrating the measured beampatterns of the antenna[26] over the opening angle of the source (see supplementary Note 1). The other contribution to the error bars on the data is given by the uncertainty in the exact beamsplitter thickness of 48 ± 2 μm.

The power as a function of frequency that arrives at the detector waveguide input can be calculated using

$$P(\nu) = \frac{c^2}{4\pi}\int_{\Omega} \frac{A(\nu)B(\nu,T_{BB})}{2\nu^2} C(\nu)G(\nu,\Omega)d\Omega, \qquad (4)$$

where c is the speed of light, Ω is the solid angle, $A(\nu)$ is the transmission of the optical elements (filters and beamsplitter), $B(\nu,T_{BB})$ is the brightness of the source given by Planck's law, $C(\nu)$ is the antenna efficiency, and $G(\nu,\Omega)$ is the antenna gain pattern. The factor $(c/\nu)^2$ reflects a single mode throughput. For the purpose of the present experiment, it is sufficient to know the relative power at each frequency. As discussed in Ref. 26, the beam patterns are measured in three frequency windows: 290–350 GHz, 640–710 GHz, and 790–910 GHz. The difference in the directivity for these bands is compensated by the difference in the part of the source that they capture. The brightness of the blackbody at the measured frequencies can be well described in the Rayleigh-Jeans limit, where $B(\nu,T_{BB}) = 2k_BT_{BB}\nu^2/c^2$, which exactly compensates the frequency dependence due to the throughput $(c/\nu)^2$. k_B is Boltzmann's constant. The antenna efficiency is the only element from Eq. (4) that introduces a frequency dependence, as shown in Figure S4 of the supplementary material.[27] Using Eq. (4), we estimate the absorbed pair-breaking power from the FTS to be 15 nW. The transmission of the optical elements $A(\nu)$ is taken into account in the correction of the measured response as explained above.

In Fig. 2, starting from 200 GHz, we observe no response until 320 GHz where the absorption rises drastically because photons have enough energy to break Cooper pairs (2Δ). This steep rise in response is partially the well-known absorption edge of the superconductor:[28] the frequency dependent absorption of a plain superconducting film through the complex sheet impedance. However, in this experiment, the antenna collects the radiation and launches it as a travelling wave into the MKID CPW. For frequencies well above the gap, it takes only 1 mm to absorb 90% of the power, thus, all power is absorbed in the detector volume. Therefore, the non-monotonous sheet resistance for frequencies above the gap does not affect the measured response in this experiment, which is crucial to make the non-equilibrium response of the superconductor visible. The percentage of the power absorbed in the CPW line is calculated using the attenuation constant of a CPW[29,30] based on the frequency dependent complex conductivity of the Ta film following Mattis and Bardeen.[8] We assume the maximum length over which radiation can be absorbed to be 10.4 mm, twice the length of the resonator. Radiation that is not absorbed (only for $h\nu < 2\Delta$) will be reemitted by the antenna. h is Planck's constant. The absorbed FTS power (15 nW) corresponds to an effective quasiparticle temperature of $T = 1$ K. However, the FTS response to this power is linear, which indicates that absorbed background power dominates N_{qp}. The minimum effective temperature consistent with this observation is 1.2 K, which we therefore take as the effective temperature in the model. It is not necessary for this temperature to be exact as η_{pb} is not strongly dependent on the bath temperature at low reduced temperatures (here $T/T_c = 0.27$).[7] T_c is the critical temperature of the superconductor. The calculated frequency dependent absorption is shown as the green dashed line in Fig. 2. The maximum around 550 GHz is due to the simulated efficiency of the antenna, which is also taken into account (see the supplementary Fig. S4).

For frequencies higher than 400 GHz, the power received by the antenna is fully absorbed in the detector waveguide. However, in Fig. 2, we observe a drop in the response close to 650 GHz (4Δ) by about a factor of two, after which the response increases again. Having taken into account all frequency dependent power contributions, the only parameter left is the frequency dependence of the non-equilibrium response of the superconductor, represented by η_{pb} in Eq. (1).

The non-equilibrium distribution of quasiparticles is calculated using a quasiparticle creation term that describes the probability of creating a quasiparticle at a certain energy by breaking a Cooper pair following Eliashberg.[5,31] In steady state, the injection of quasiparticles at that energy is balanced by electron-phonon interaction (scattering and recombination). The kinetic equations for the non-equilibrium quasiparticle- and phonon energy distributions are solved following the approach by Chang and Scalapino.[6] The numerical procedure is explained in Ref. 32. The resulting distribution functions $f(E)$ *for constant absorbed power* are shown for various frequencies in Fig. 3(a). For higher excitation frequencies, there are more quasiparticles with a higher

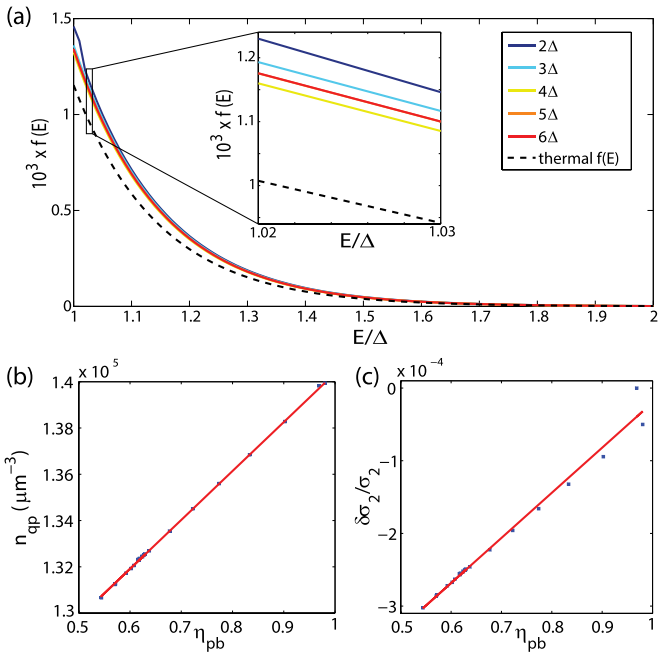

FIG. 3. (a) The calculated quasiparticle distribution functions $f(E)$ as a function of energy for different excitation energies (2Δ, 3Δ, 4Δ, 5Δ, and 6Δ). The lines for 5Δ and 6Δ coincide. The absorbed power was kept constant and the resulting variation is thus only an effect of the frequency of the absorbed photons. The inset highlights the differences in $f(E)$ on a small energy scale. (b) The change in the quasiparticle density (n_{qp}) and (c) the imaginary part of the complex conductivity $\delta\sigma_2/\sigma_2$ as a function of the pair breaking efficiency η_{pb}. The different points are calculated at different excitation frequencies, 320–1100 GHz. The red lines are linear fits to the simulated points.

energy, and therefore less weight close to the gap, where the resonator is sensitive. We therefore expect the maximum resonator signal at $\nu = 2\Delta/h$ and a minimum at $\nu = 4\Delta/h$. The pair breaking efficiency, η_{pb}, calculated from these distribution functions is shown in Fig. 2 (blue dashed-dotted line). When multiplied with the calculated frequency dependent absorption (red line) it clearly describes the main shape of the measured response.

It was shown by Guruswamy *et al.*[7] that the behaviour of $f(E)$ for frequencies higher than $\nu = 4\Delta/h$ crucially depends on the phonon trapping factor. When phonons are released due to scattering or recombination, the ratio of their escape time τ_{esc} and the pair-breaking time τ_{pb} determines how many quasiparticles can be generated from a single incoming photon. Only for $\tau_{esc}/\tau_{pb} > 1$ can η_{pb} increase at energies above 4Δ. τ_{pb} is material dependent and equals 2.3×10^{-11} s for Ta[33] (2.8×10^{-10} s for Al). For 200 nm Ta on Si we obtain $\tau_{esc} = 2$ ns,[34] which gives a trapping factor of 87, which makes Ta a favourable choice (over, e.g., Al) to experimentally address the effect of phonon trapping. It is difficult to estimate the precise trapping factor because the substrate is a relatively thin membrane and because of the Nb seed layer, but it is certainly large. In practice, η_{pb} is the same for trapping factors of 15 and higher.[7] The rise in η_{pb} above $h\nu = 4\Delta$, which is due to phonon trapping and which we observe in Fig. 2, qualitatively distinguishes the non-equilibrium response from other frequency dependent phenomena.

When Cooper pairs are broken, the created high energy quasiparticles relax back to energies close to the gap on a timescale of 0.1–10 ns.[20] The response can well be described by an effective number of quasiparticles N_{qp} using η_{pb} as in Eq. (1).[7] From the calculated $f(E)$, we derive η_{pb}, n_{qp} (quasiparticle density), and σ_2. The (almost) linear relationship between those properties (Eq. (1)) is demonstrated in Figures 3(b) and 3(c). These figures and Eq. (1) suggest that a simple effective N_{qp} could explain the data, but this would only hold for a single excitation frequency.[22,35,36] We emphasize that the knowledge of the microscopic $f(E)$ is needed to obtain the correct N_{qp} at a certain (P, ν) through η_{pb}, to ultimately explain the frequency dependence of our observations in Fig. 2.

The qualitative agreement between measurement and simulation in Fig. 2 is very good, especially the peak around 2Δ and the characteristic 4Δ point are well represented. The deviation that occurs at higher frequencies is most likely due to an incomplete understanding of the combination of the FTS system with the lens-antenna. Except for the mentioned uncertainties, the antenna efficiency and absorption length are not independently measured and the removal of the residual ripple in the response is not exact. To get a deviation smaller than the 10%–15% achieved now, one would need a complicated calibration with a bolometer with better sensitivity than the Ta MKID coupled to the same lens-antenna. We note that the characteristic impedance of the CPW (Z_0) is also frequency dependent, but it changes the power transmitted from antenna to waveguide by only 0.1%. The diffusion length of quasiparticles in Ta is 2 μm based on a recombination time of 50 ns (for an effective temperature of 1.2 K) and a diffusion constant of 0.8 cm^{2}s^{-1} (Refs. 37 and 38 and the measured resistivity). The effect of diffusion of quasiparticles from the central strip at the antenna feed is therefore negligible. Furthermore, we checked that for this CPW geometry radiation losses are a factor 10 lower than absorption in the superconductor.[39]

The measured energy gap in the FTS response occurs at 324 GHz, corresponding to a T_c of 4.4 K, assuming $2\Delta = 3.52 k_B T_c$. This is consistent with the minimum response in Fig. 2 at around 650 GHz (4Δ). However, the DC-measured T_c of this film is 4.77 K, although most of our previous Ta films have also shown a T_c of 4.4 K.[40] We presume that the Nb seed layer is thicker than anticipated giving a thin layer with a somewhat higher T_c dominating the DC transport, whereas the radiation absorption is dominated by the lower gap in the thick Ta top layer.

The microwave readout power can strongly affect the response of a microwave resonator.[16,32] In this experiment, we can neglect effects due to the absorbed readout power (1.8 nW), which is much smaller than the absorbed pair-breaking signal. Readout power effects are only expected in the opposite limit,[41] which is, nevertheless, important to investigate in the future. The observed agreement of the measurements with the model is encouraging. At the same time, it underlines the importance of understanding and controlling these parameters to optimise superconducting detectors.

We would like to thank Jan Barkhof for help with the FTS calibration. This work was in part supported by ERC starting Grant Nos. ERC-2009-StG and 240602 TFPA. T. M. Klapwijk acknowledges financial support from the Ministry of Science and Education of Russia under Contract No.

14.B25.31.0007 and from the European Research Council Advanced Grant No. 339306 (METIQUM). P. J. de Visser acknowledges support from a Niels Stensen Fellowship.

[1]P. K. Day, H. G. LeDuc, B. A. Mazin, A. Vayonakis, and J. Zmuidzinas, Nature **425**, 817 (2003).
[2]A. Peacock, P. Verhoeve, N. Rando, A. van Dordrecht, B. G. Taylor, C. Erd, M. A. C. Perryman, R. Venn, J. Howlett, D. J. Goldie, J. Lumley, and M. Wallis, Nature **381**, 135 (1996).
[3]P. M. Echternach, K. J. Stone, C. M. Bradford, P. K. Day, D. W. Wilson, K. G. Megerian, N. Llombart, and J. Bueno, Appl. Phys. Lett. **103**, 053510 (2013).
[4]A. Rothwarf and B. N. Taylor, Phys. Rev. Lett. **19**, 27 (1967).
[5]B. I. Ivlev, S. G. Lisitsyn, and G. M. Eliashberg, J. Low Temp. Phys. **10**, 449 (1973).
[6]J.-J. Chang and D. Scalapino, J. Low Temp. Phys. **31**, 1 (1978).
[7]T. Guruswamy, D. J. Goldie, and S. Withington, Supercond. Sci. Technol. **27**, 055012 (2014).
[8]D. C. Mattis and J. Bardeen, Phys. Rev. **111**, 412 (1958).
[9]J. Zmuidzinas, Annu. Rev. Condens. Matter Phys. **3**, 169 (2012).
[10]S. J. C. Yates, J. J. A. Baselmans, A. Endo, R. M. J. Janssen, L. Ferrari, P. Diener, and A. M. Baryshev, Appl. Phys. Lett. **99**, 073505 (2011).
[11]R. M. J. Janssen, J. J. A. Baselmans, A. Endo, L. Ferrari, S. J. C. Yates, A. M. Baryshev, and T. M. Klapwijk, Appl. Phys. Lett. **103**, 203503 (2013).
[12]R. M. J. Janssen, J. J. A. Baselmans, A. Endo, L. Ferrari, S. J. C. Yates, A. M. Baryshev, and T. M. Klapwijk, Proc. SPIE **9153**, 91530T (2014).
[13]P. J. de Visser, J. J. A. Baselmans, J. Bueno, N. Llombart, and T. M. Klapwijk, Nat. Commun. **5**, 3130 (2014).
[14]P. D. Mauskopf, S. Doyle, P. Barry, S. Rowe, A. Bidead, P. A. R. Ade, C. Tucker, E. Castillo, A. Monfardini, J. Goupy, and M. Calvo, J. Low Temp. Phys. **176**, 545 (2014).
[15]J. Hubmayr, J. Beall, D. Becker, H.-M. Cho, M. Devlin, B. Dober, C. Groppi, G. C. Hilton, K. D. Irwin, D. Li, P. Mauskopf, D. P. Pappas, J. Van Lanen, M. R. Vissers, Y. Wang, L. F. Wei, and J. Gao, Appl. Phys. Lett. **106**, 073505 (2015).
[16]P. J. de Visser, D. J. Goldie, P. Diener, S. Withington, J. J. A. Baselmans, and T. M. Klapwijk, Phys. Rev. Lett. **112**, 047004 (2014).
[17]R. M. J. Janssen, A. Endo, P. J. de Visser, T. M. Klapwijk, and J. J. A. Baselmans, Appl. Phys. Lett. **105**, 193504 (2014).
[18]P. J. de Visser, J. J. A. Baselmans, P. Diener, S. J. C. Yates, A. Endo, and T. M. Klapwijk, Phys. Rev. Lett. **106**, 167004 (2011).
[19]M. Kurakado, Nucl. Instrum. Methods **196**, 275 (1982).
[20]A. G. Kozorezov, A. F. Volkov, J. K. Wigmore, A. Peacock, A. Poelaert, and R. den Hartog, Phys. Rev. B **61**, 11807 (2000).
[21]F. Jaworski and W. H. Parker, Phys. Rev. B **20**, 945 (1979).
[22]A. D. Smith, W. J. Skocpol, and M. Tinkham, Phys. Rev. B **21**, 3879 (1980).
[23]K. E. Kornelsen, M. Dressel, J. E. Eldridge, M. J. Brett, and K. L. Westra, Phys. Rev. B **44**, 11882 (1991).
[24]M. Dressel, Adv. Condens. Matter Phys. **2013**, 104379 (2013).
[25]A. Neto, IEEE Trans. Antennas Propag. **58**, 2238 (2010).
[26]A. Neto, N. Llombart, J. J. A. Baselmans, A. Baryshev, and S. J. C. Yates, IEEE Trans. Terahertz Sci. Technol. **4**, 26 (2013).
[27]See supplementary material at http://dx.doi.org/10.1063/1.4923097 for the setup corrections applied to the raw FTS response and simulations of the absorbed power in the CPW and the antenna efficiency.
[28]R. E. Glover and M. Tinkham, Phys. Rev. **108**, 243 (1957).
[29]C. L. Holloway and E. F. Kuester, IEEE Trans. Microwave Theory Tech. **43**, 2695 (1995).
[30]P. de Visser, "Quasiparticle dynamics in aluminium superconducting microwave resonators," Ph.D. dissertation (Delft University of Technology, 2014).
[31]G. M. Eliashberg, JETP Lett. **11**, 114 (1970), available at http://www.jetpletters.ac.ru/ps/1716/article_26086.shtml.
[32]D. J. Goldie and S. Withington, Supercond. Sci. Technol. **26**, 015004 (2013).
[33]S. B. Kaplan, C. C. Chi, D. N. Langenberg, J. Chang, S. Jafarey, and D. J. Scalapino, Phys. Rev. B **14**, 4854 (1976).
[34]S. B. Kaplan, J. Low Temp. Phys. **37**, 343 (1979).
[35]J. Gao, J. Zmuidzinas, A. Vayonakis, P. Day, B. Mazin, and H. Leduc, J. Low Temp. Phys. **151**, 557 (2008).
[36]G. Catelani, L. I. Glazman, and K. E. Nagaev, Phys. Rev. B **82**, 134502 (2010).
[37]S. Friedrich, K. Segall, M. C. Gaidis, C. M. Wilson, D. E. Prober, A. E. Szymkowiak, and S. H. Moseley, Appl. Phys. Lett. **71**, 3901 (1997).
[38]T. Nussbaumer, P. Lerch, E. Kirk, A. Zehnder, R. Füchslin, P. F. Meier, and H. R. Ott, Phys. Rev. B **61**, 9719 (2000).
[39]M. Frankel, S. Gupta, J. Valdmanis, and G. Mourou, IEEE Trans. Microwave Theory Tech. **39**, 910 (1991).
[40]R. Barends, S. van Vliet, J. J. A. Baselmans, S. J. C. Yates, J. R. Gao, and T. M. Klapwijk, Phys. Rev. B **79**, 020509(R) (2009).
[41]T. Guruswamy, D. J. Goldie, and S. Withington, Supercond. Sci. Technol. **28**, 054002 (2015).